Detergentless Water/Oil Microemulsions: IV. The Ternary Pseudo-phase Diagram for and Properties of the System Toluene/2-Propanol/Water

G. LUND and S.L. HOLT,[1] Department of Chemistry, University of Georgia, Athens, GA 30602

ABSTRACT

The ternary-pseudo phase diagram for toluene, water and 2-propanol has been constructed from conductivity measurements. Several structured regions have been identified and region boundaries confirmed by carbon-13 nuclear magnetic resonance spectroscopy. Prominent among the structured pseudo-phases is a region of water dispersed microemulsions. Preliminary light scattering data suggest a droplet diameter of 50-300 Å.

INTRODUCTION

The ternary diagram for various compositions of hexane, 2-propanol and water has been investigated by conductivity, ultracentrifugation and proton magnetic resonance spectroscopy (1,2). Regions of differing liquid structure were identified, one of which consists of detergentless microemulsions (1). The effect of the addition of detergent (1), sodium chloride (2) and potassium hydroxide (3), has been ascertained. The utility of detergentless microemulsions as media for chemical reactions has been demonstrated through the study of base-catalyzed hydrolysis of long chain esters (3), the metalation of prophyrins (4) and studies of the complexation of Cu(II) with the side chains of amino acids (5).

In an effort to expand the number of known ternary systems which produce detergentless microemulsions and to provide some insight into both the statics and dynamics of microemulsification, we have investigated the ternary system toluene/2-propanol/water. Regions of differing liquid structure, analogous to those characteristic of the hexane/2-propanol/water systems, have been identified by conductivity and ^{13}C nuclear magnetic resonance (NMR) spectroscopy. Ultracentrifugation has been used to define the boundary between the turbid unstable macroemulsion region and the stable microemulsion region. In addition, the microemulsion region has been further defined by preliminary light scattering studies.

EXPERIMENTAL

Reagent-grade toluene and 2-propanol were treated by passage through a column of 60-200 mesh silica gel followed by distillation onto washed 4-Å molecular sieves. Immediately prior to use, the 2-propanol was redistilled in order to obtain a conductivity of less than 0.02 μmho/cm. Deionized water was twice distilled from a Pyrex still with the exception of that used for conductivity measurements, which was distilled only once after deionization so that it retained a reasonable residual conductivity.

Conductivity measurements were made with a Yellow Springs Instrument Co., Inc. (YSI) Model 31 null reading conductivity bridge using a YSI 3402 insertion type cell (k=0.1). The cell electrodes were replatinized after each 20 hr of use. Ternary solution structure diagrams were constructed by titrating, with 2-propanol, 10 ml of toluene containing an aliquot of water. Conductivity readings were taken after each addition of alcohol, as described in earlier work (1,2).

^{13}C NMR spectra were recorded on a JEOL-PFT-100 spectrometer. Chemical shifts were measured relative to an external tetramethylsilane reference enclosed in a capillary and inserted into a D_2O lock capillary which was in turn inserted into the sample. Bulk diamagnetic corrections were made by comparing the resonance of an internal reference of *p*-dioxane in a sample to that of pure *p*-dioxane (67.40 δ). Toluene/2-propanol/H_2O samples used for the ^{13}C NMR experiment consisted of compositions lying on lines of constant mole fraction of water (Fig. 1), and were prepared in a manner analogous to that described in previous work (2).

A Brice-Phoenix (Series 2000) light scattering spectophotometer using the 436 nm and 546 nm wavelengths of a mercury vapor source was used for the light scattering studies. All samples were clarified prior to measurement by passage through a 0.8-micron pore diameter pressure filter. As in the NMR experiment, sample compositions were chosen so as to represent solutions containing a constant mole fraction of water. Spectrophotometer readings were recorded by monitoring photomultiplier output voltage

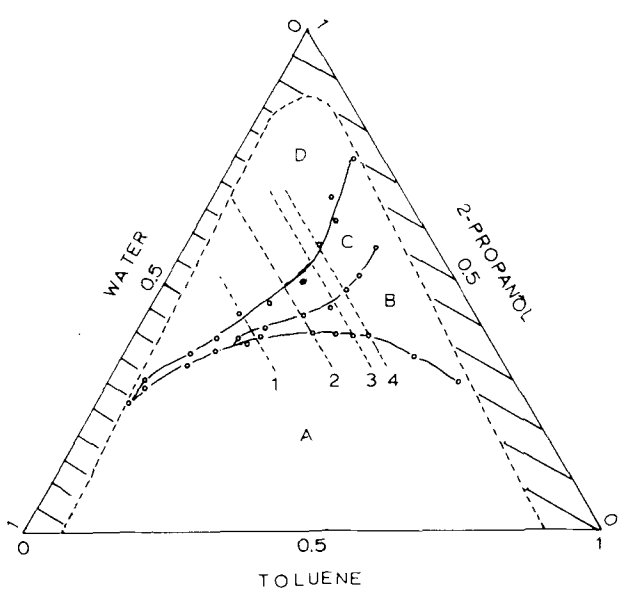

FIG. 1. Ternary pseudo-phase diagram for toluene/water/2-propanol, lines 1, 2, 3, 4 represent H_2O isopleths of 0.4, 0.3, 0.23 and 0.2, respectively.

[1] Author to whom correspondence should be addressed.

on a Kiethley Model 160 digitial multimeter.

Ultracentrifugation studies were performed with a Beckman L2-65B preparative ultracentrifuge employing a Type Ti-65 rotor at 55,000 rpm using polyallomer or nitrocellulose tubes. The turbid macroemulsion/stable microemulsion phase boundary was identified by observing, in samples of increasing 2-propanol concentration, the point at which phase separation no longer occurred upon centrifugation.

RESULTS

Conductivity

The ternary pseudo-phase diagram which was constructed for toluene/2-propanol/water based on conductivity measurements appears in Figure 1. Plots of measured conductivity vs mole fraction of 2-propanol the solution consistently exhibited behavior similar to those observed for compositions of hexane/2-propanol/H_2O (1). For compositions on the right side of the pseudo-phase diagram there is a linear increase in conductivity beginning at point a on Figure 2; the boundary between regions A and B, and continuing to the point of inflection, b, which defines the B/C boundary. The conductivity continues to increase, though more slowly, to point c, the C/D boundary, where it begins to decrease.

As we move across the phase diagram from right to left, i.e., to higher water concentrations, conductivity measurements show a decrease in the area of region B until it disappears entirely. The same behavior is observed for region C.

^{13}C NMR

^{13}C NMR spectra were recorded for samples lying on 3 different lines of constant mole fraction of water, indicated by lines 1, 2 and 4 in Figure 1. The widths of the resonances, measured at half height for the methine carbon of the 2-propanol and the methyl carbon of toluene are plotted in Figure 3 as a function of the mole fraction of 2-propanol in the samples. The samples from which these particular data are obtained lie on a line of constant mole fraction of water of 0.2 (line number 4 in Fig. 1). Figure 3a describes the behavior of the methine carbon of the 2-propanol whereas Figure 3b illustrates the behavior of the toluene methyl carbon. In both cases only one resonance is observed, implying that within the level of detection of the instrument, one average environment exists for both the 2-propanol and the toluene. The inflections exhibited in both figures coincide with the region boundaries shown in Figure 1. The ^{13}C resonances for the remaining carbons of the 2-propanol and toluene molecules behave similarly but the effect is not as pronounced. As a general statement, the ^{13}C resonance widths for the 2-propanol exhibit a narrowing when solution compositions transit a region boundary whereas the resonance widths for the toluene molecule broaden.

Light Scattering

The intensity of light scattered at 90° was measured for several compositions of toluene/2-propanol/water. These samples lie on the lines of constant mole fraction of water of 0.23 and 0.3 (lines 2 and 3 in Fig. 1a). Values of F(Gs/Gws) at both 436 nm and 546 nm were determined for each sample by calculating the ratio of the voltmeter reading at 0° to that at 90°. Thus, this quantity is proportional to the turbidity of the sample.

Plots of the value F(Gs/Gws) vs mole fraction of 2-propanol contained in the sample appear in Figure 4. As expected, the turbidity decreases with increasing 2-propanol, but exhibits a local maximum at the C/D boundary for both $\bar{X}_{H_2O} = 0.23$ and $\bar{X}_{H_2O} = 0.3$. An additional local maximum was observed at the B/C boundary in the $\bar{X}_{H_2O} = 0.23$ series. The scattered intensity continues to decrease past the C/D boundary until it approaches that observed for a 40% solution of toluene in 2-propanol. Measurement of the angular dependence of the turbidity from 40° to 140° as well as the depolarization of the scattered radiation indicates no observable dissymmetry. In addition, average values of calculated turbidities measured at 546 nm com-

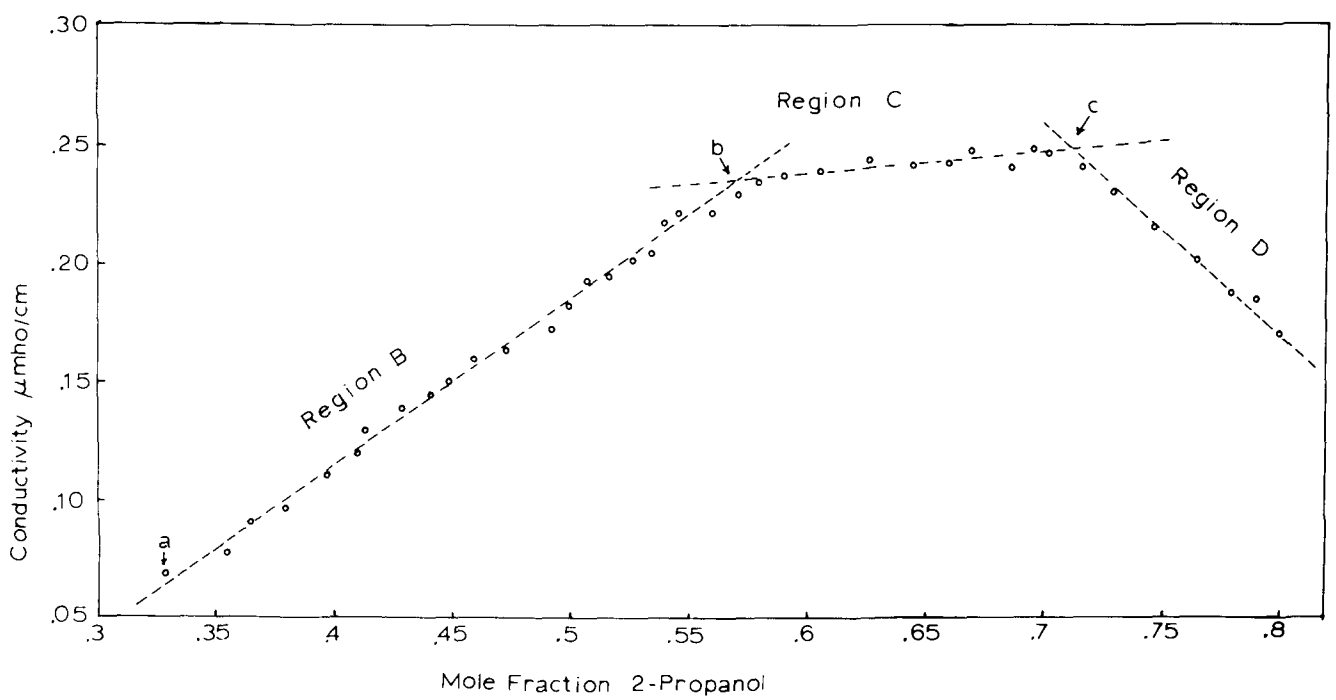

FIG. 2. Plot of conductivity vs mole fraction of 2-propanol for 0.5 mL H_2O in 10 mL toluene titrated with 2-propanol. Point a represents the A/B region boundary whereas points b and c are the B/C and C/D region boundaries, respectively.

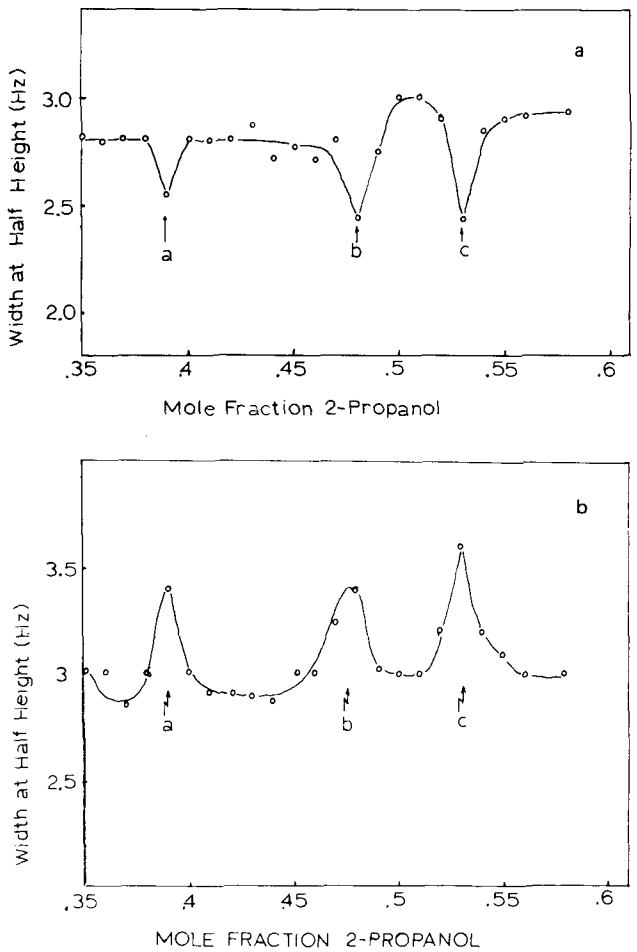

FIG. 3. (a) Plot of ^{13}C NMR peak width at half-height vs mole fraction 2-propanol methine carbon. (b) Peak width at half-height for toluene methyl carbon vs mole fraction 2-propanol. In both a and b the solutions lie on the 0.2 $\bar{X}_{H_2O}$ line labeled line 4 in Figure 1. Points a, b and c correspond to region boundaries A/B, B/C, C/D, respectively, in both cases.

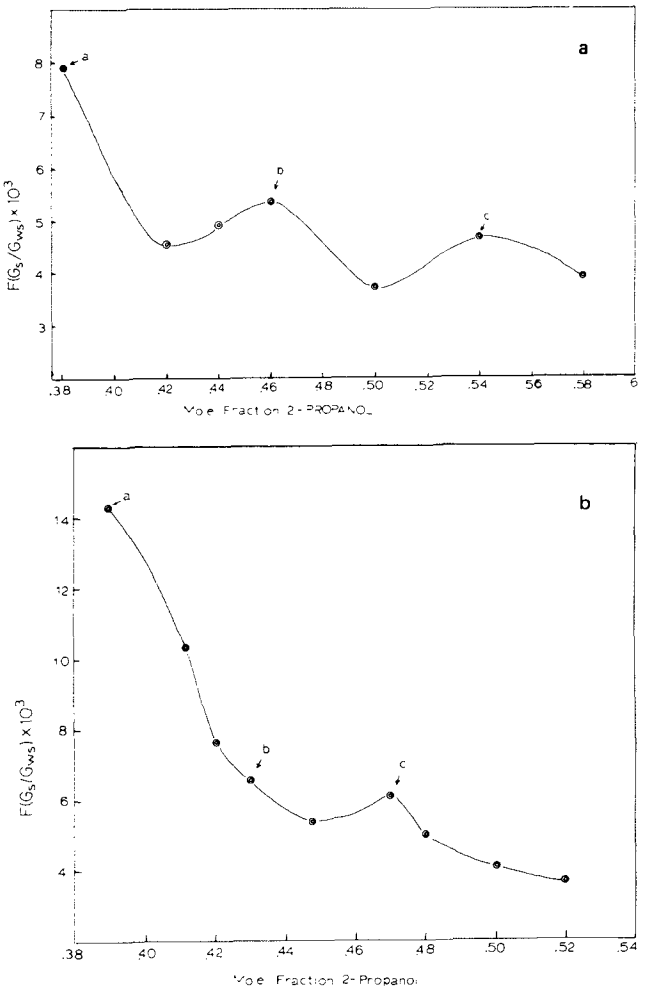

FIG. 4. Plots of light scattering ratio $F(G_{rs}/G_{rws})$ vs mole fraction of 2-propanol. Figure 4a is for solutions lying on the 0.23 x H_2O line (line 3 in Fig. 1). In both figures, points a, b and c correspond to the A/B, B/C and C/D region boundaries, respectively.

pared to those measured at 436 nm demonstrated a $1/\lambda^4$ dependence in accordance with Rayleigh scattering behavior for small spheres.

DISCUSSION

As observed in previous work on ternary solutions of hexane/2-propanol/water, there are 4 detectable regions in the ternary pseudo-phase diagram for compositions of toluene/2-propanol/water (1,2). (The term "pseudo-phase" is used to denote that, though the 4 regions of the ternary diagram represent solutions of physically distinct character, these regions are not necessarily distinct phases as defined by the phase rule.) In analogy with the earlier work, the regions as identified by conductivity are as follows. Ternary compositions from region A are turbid macroemulsions when freshly prepared or agitated which, upon standing or when subjected to centrifugation eventually break into 2 phases. Compositions which constitute the remainder of the ternary diagram are homogeneous to the naked eye, optically transparent and show no phase separation after months of standing undisturbed. Conductivity, NMR and light scattering measurements locate 3 regions in this portion of the pseudo-phase diagram.

The rise in conductivity throughout the microemulsion region suggests that the ionic species contained in the aqueous phase are experiencing increased mobility as 2-propanol is added to the solution. This behavior can be rationalized if we assume the water is dispersed as small droplets, which diminish in size and increase in number as the concentration of 2-propanol increases. This results in a corresponding increase in the number of charge carriers and a subsequent rise in the conductivity.

Eventually, the water is dispersed into small enough aggregates that a discrete droplet with bulk encapsulated water is no longer the thermodynamically preferred arrangement. At this point b, a sharp transition to small hydrogen-bonded aggregates of 2-propanol and water occurs. These aggregates evidently become smaller and more mobile in much the same manner as the microemulsion until a true ternary solution (region D) containing no apparent microheterogeneity is attained. At this point the conductivity trails off as the solution becomes diluted by the nonconducting 2-propanol.

Corroboration of this view can be obtained from the light scattering data. Ignoring the local maxima at the phase boundaries, the curves of Figure 4 are reminiscent of those observed for turbidity vs concentration curves for micellar solutions. The presence of significant excess turbidities above those resulting from solutions of 2 component mixtures indicates the presence of definite microheterogeneity in the B and C regions. This observation, coupled with the lack of any observable dissymmetry or depolarization, lends support to the concept that regions B and

C contain small isotropic centers whose refractive index and density differs from that of continuous phase. The fact that the scattered radiation follows Rayleigh behavior indicates that the droplets have a radius of less than 1/15 of the incident radiation wavelengths. Although it was not possible to perform meaningful particle size calculations from the observed turbidities because of the ternary nature of the system, rough estimation leads us to believe that in the B region, the droplet diameters range from a lower limit of 50 Å to an upper limit of 300 Å.

Data on chemical reactivity in these systems also support the concepts of a distinct interphase in region B which no longer exists in region C. Studies on the rate of Cu(II) incorporation into *meso*-tetraphenylprophine ($TPPH_2$) are markedly affected by solvent composition. Since the Cu(II) ion is soluble only in the aqueous droplet whereas the $TPPH_2$ is only oil soluble, the rate of the reaction is highly interphase-dependent (6). When the reaction medium is taken from the microemulsion region of the ternary pseudophase diagram the rate of metalation is fairly constant: $\sim 7 \times 10^{-3}$/hr. However, when the reaction is carried out in region C the rate of reaction increases at an almost exponential rate as a function of 2-propanol concentration, indicating a breakdown of the interphase.

Further insight into both the statics and dynamics of microemulsion structure can be obtained from the ^{13}C NMR data. Focusing our attention on Figures 3a and 3b we note the contrasting behavior of the ^{13}C NMR resonance widths of the 2-propanol and the toluene as region boundaries are traversed. The narrowing of the 2-propanol resonances at the region boundaries indicates an enhanced alcohol mobility whereas the broadening of the toluene signals suggests a restriction of molecular motion. Relative resonance widths also indicate that the 2-propanol mobility is somewhat less in the C and D regions than it is in the microemulsion region. These data can be rationalized within the framework of our model (3). In the microemulsion region, the predominant location of the 2-propanol is in the interphase between the bulk encapsulated water and the toluene continuum. Here the interactions are primarily alcohol-alcohol although some 2-propanol/water H-bonding undoubtedly occurs (2). Toluene/2-propanol interaction is not a factor. In regions C and D, aggregate sizes are considerably smaller, leading to enhanced 2-propanol/water H-bonding. Structures in all 3 regions are relatively rigid by virtue of the H-bonding but become more dynamic while transiting from one structure to another. This permits an increase in toluene/2-propanol/water H-bonding, decreasing the toluene mobility.

The appearance of local maxima in the light scattering curves of Figure 4 tend to support the presence of long range order. A change from small droplet structure to that of extensive water/2-propanol/toluene interactions could result in large areas of density fluctuations in the sample with a concurrent increase in the scattering intensity. When sufficient 2-propanol has been added to the system to permit a new structure to form, the water/alcohol interactions once again predominate, allowing normal mobility for the toluene. Thus the resonance widths as well as the light scattering intensity decrease.

ACKNOWLEDGMENTS

The authors thank Mark J. Stewart for technical assistance. The work was supported in part by NSF Grant CHE 7913802.

REFERENCES

1. G.D. Smith, C.E. Donelon and R.E. Barden, J. Colloid Interface Sci. 60:488 (1977).
2. B.A. Keiser, D. Varie, R.E. Barden and S.L. Holt, J. Phys. Chem. 83:1276 (1979).
3. N. Borys, S.L. Holt and R.E. Barden, J. Colloid Interface Sci. 71:526 (1979).
4. B.A. Keiser, R.E. Barden and S.L Holt, Ibid. 73:290 (1980).
5. G.D. Smith, R.E. Barden and S.L. Holt, J. Coord. Chem., 8:157 (1978).
6. B.A. Keiser and S.L. Holt, in preparation.

[Received October 16, 1979]